Supplementary Information File for:

Nanocomposite of CeO_2 and high-coercivity magnetic carrier with large specific surface area

Alice Reznickova Mantlikova[a], Jiri Plocek[b], Barbara Pacakova[a], Simona Kubickova[a], Ondrej Vik[b], Daniel Niznansky[c], Miroslav Slouf[d] and Jana Vejpravova[a*]

[a] *Institute of Physics of the CAS, Department of Magnetic Nanosystems, Na Slovance 2, 182 21 Praha 8, Czech Republic*

[b] *Institute of Inorganic Chemistry of the CAS., Husinec – Rez 1001, 250 68 Rez, Czech Republic*

[c] *Charles University in Prague, Department of Inorganic Chemistry, Faculty of Science, Hlavova 2030/8, 128 43 Prague 2, Czech Republic*

[d] *Institute of Macromolecular Chemistry, Academy of Sciences of the Czech Republic, Heyrovsky Sq. 2, 162 06 Prague 6, Czech Republic*

[*]corresponding author - email: vejpravo@fzu.cz,

Energy Dispersive X-Ray Analysis (EDX)

Table S1: Results of the EDX analysis: Ce, Fe, Co and S atomic content and calculated Fe/Co ratios. *at* is the abbreviation for atomic %.

Sample	Ce (at %)	Fe (at %)	Co (at %)	S (at %)	Fe/Co
Co_free	-	30.9	12.6	-	2.5
Co_mod	-	36.2	9.7	-	3.7
v02	29.3	6.1	1.6	4.3	3.7
v03	28.8	5.9	1.5	1.6	4.1
v04	33.4	5.2	1.5	0.4	3.6
v05	33.0	6.3	1.5	1.2	4.2
v06	29.6	6.3	1.6	-	3.9

The low intensity of the Co peak in the EDX spectrum (consequence of small amount of Co in the samples) together with the large charging of the samples during EDX measurements result in larger experimental error of the determined values of the Co content in the nanocomposite samples in comparison with the Co_free and Co_mod samples. Thus, the resulting Fe/Co ratios of nanocomposite samples are determined within the experimental error of 0.5.

Moreover, small amount of sulfur was also detected in all samples except v06, as a residuum of the sulfuric acid used in the NP incorporation process.

Transmission Electron Microscopy (TEM)

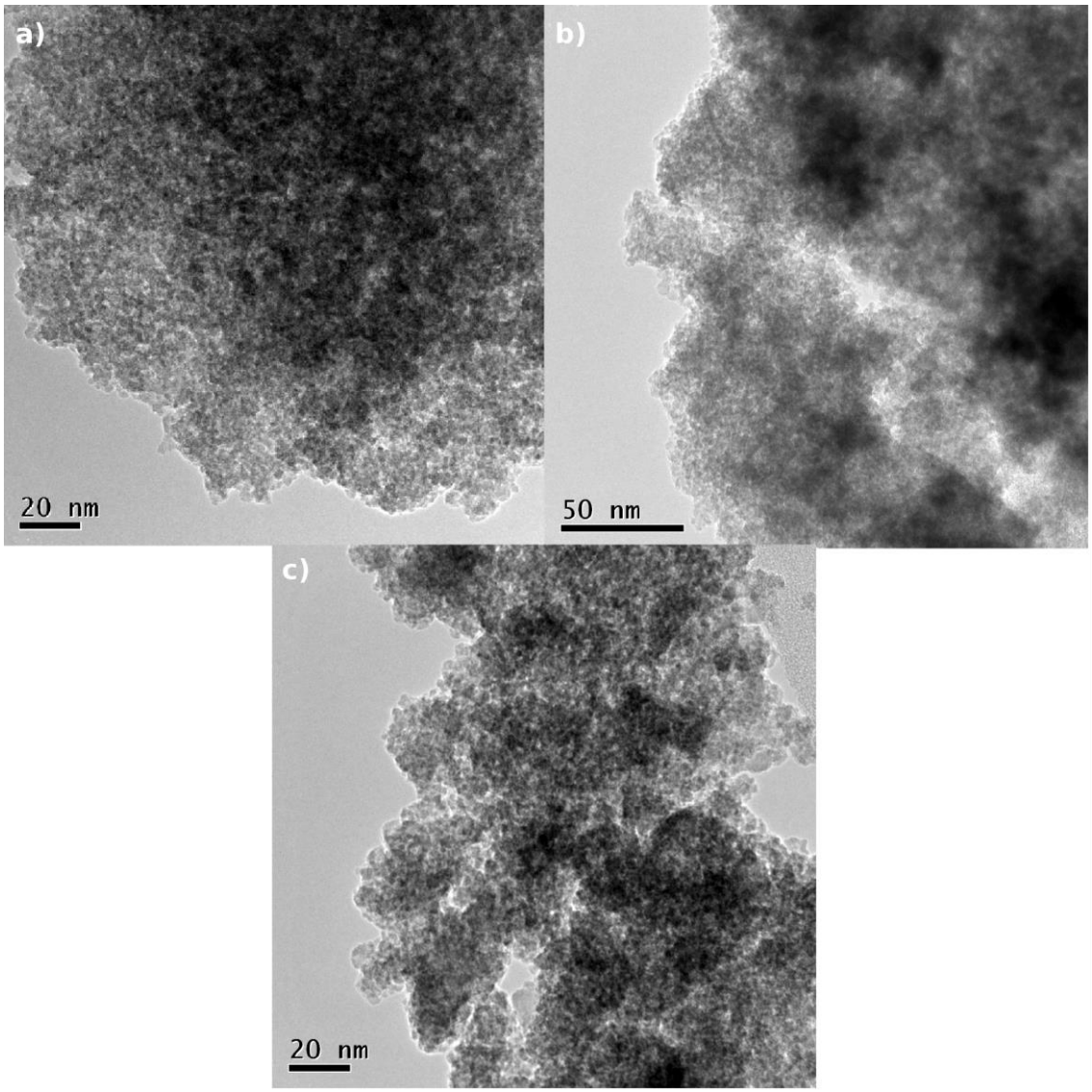

Figure S1: The TEM images of the (a) v03, (b) v04 and (c) v05 samples.

Mössbauer Spectroscopy

Table S2: The Mossbauer parameters of the samples: the isomer shift, δ, the quadrupolar shift, 2ε, hyperfine field, B_{hf}, FWHM with the distribution of the B_{hf}, Dist.:

	δ (mm.s^{-1})	**2 ε (mm.s^{-1})**	**B_{hf} (T)**	**FWHM/Dist. (mm.s^{-1})/(T)**	**Rel. area (%)**	**Interpr.**
Unmodified sample (CoFe_free)						
Subsp. 1 (Fe^{3+} T_d)	0.34	-0.05	43.1	0.46/6.1	52.4	Fe^{3+} blocked
Subsp. 2 (Fe^{3+} O_h)	0.31	0.00	47.2	0.44/1.7	34.0	Fe^{3+} blocked
Subsp. 3 (Fe^{3+} para)	0.33	0.77	-	0.90	13.6	Fe^{3+} SPM
Subsp. 4 (Fe^{3+} near T_B)	0.41	-	-	11.84	-	Fe^{3+} near T_B
Modified sample (CoFe_mod)						
Subsp. 1 (Fe^{3+} T_d)	0.34	-0.05	43.0	0.44/6.8	45.4	Fe^{3+} blocked
Subsp. 2 (Fe^{3+} O_h)	0.31	0.00	47.3	0.44/1.9	31.2	Fe^{3+} blocked
Subsp. 3 (Fe^{3+} para)	0.35	0.75	-	0.86	23.4	Fe^{3+} SPM
Subsp. 4 (Fe^{3+} near T_B)	0.36	-	-	10.80	-	Fe^{3+} near T_B

The spectra of the CoFe_free and CoFe_mod samples were refined with two sextets corresponding to the Fe^{3+} ions, the ratio of relative areas were not fixed. The distribution of the B_{hf} was used to fit the spectra. The subspectra labels in Table S2 correspond with the notation in the main manuscript body.

The spectra of the nanocomposite samples were not refined. The low relative mass of the $CoFe_2O_4$ in the sample and high absorption of the cerium caused that the measured spectra did not have sufficient quality for proper analysis (see example spectrum at Figure S2).

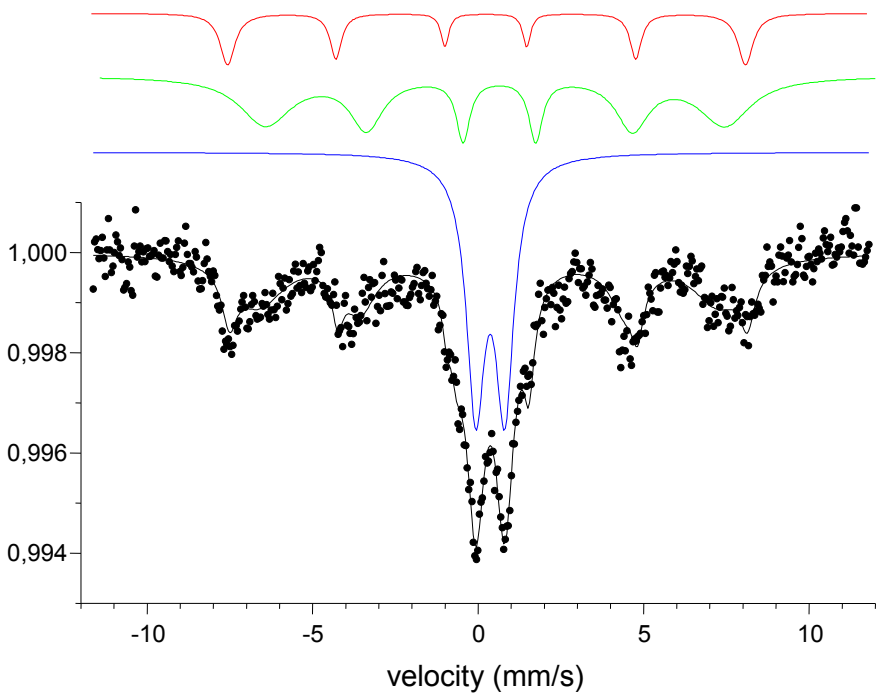

Figure S2: Mössbauer spectra of the v06 sample measured at RT. Blue line corresponds to the $CoFe_2O_4$ NPS in SPM state, green and red lines correspond to the octahedral and tetrahedral sites in spinel structure, respectively for the $CoFe_2O_4$ NPs in the blocked state.

ZFC curve refinement – a useful tool for determination of the distribution of blocking temperatures

The ZFC magnetization of a system of NPs is given by equation [1-3]:

$$M_{ZFC}(T) \propto \frac{M_S^2 H_m}{3K_{eff}}\left[\frac{25}{t}\int_0^t t_B f(t_B)dt_B + \int_t^\infty f(t_B)dt_B\right], \quad (1)$$

where the first contribution is contribution from the SPM NPs and second is from NPs in the blocked state. M_S is the saturation magnetization; K_{eff} is the effective anisotropy constant of NPs, H_m is magnetic field used for ZFC measurement (0.01 T for all samples) and t corresponds to the reduced temperature, $t = T/T_{Bm}$. The $f(t_B)$ is a log-normal distribution of the reduced blocking temperatures, $t_B = T_B/T_{Bm}$ defined as:

$$f(t_B) = \frac{1}{\sqrt{2\pi}\sigma}\frac{1}{t_B}\exp\left(-\frac{\ln^2 t_B}{2\sigma^2}\right), \quad (2)$$

with T_{Bm} representing median blocking temperature and σ corresponding to the distribution width. For purpose of our refinement, we adapted equation (1) as:

$$M_{ZFC}(T) \propto C + \frac{M_S^2 H_m}{3K_{eff}}\left[\frac{25}{t}\int_0^t t_B f(t_B)dt_B + \int_t^\infty f(t_B)dt_B\right], \quad (3)$$

where C is a scaling factor used due to the random orientation of the freezing moments resulting to the unpredictable nonzero value of the low temperature magnetization. Refinement procedure was done in the Octave/Matlab software. Mean blocking temperatures, T_{B_mean} were calculated for all samples using the well-known relation between median, distribution width and mean value of the log-normal distribution:

$$T_{B\_mean} = T_{Bm}\exp\left(\frac{\sigma^2}{2}\right). \quad (4)$$

Example of the fit for the v06 sample is displayed in Figure S3 and resulting values of the T_{bm} and σ obtained for all samples are summarized in Table S2.

Table S2: Results of the *ZFC* curves refinement: median blocking temperature, T_{b_m} and width of the distribution of the blocking temperatures, σ.

Sample	T_{Bm} **(K)**	**σ**
Co_free	165.1 ± 1.3	0.42 ± 0.01
Co_mod	173.2 ± 2.1	0.67 ± 0.02
v02	185.7 ± 1.6	0.63 ± 0.01
v03	187.5 ± 1.9	0.64 ±0.01
v04	186.6 ± 1.0	0.63 ± 0.01
v05	194.4 ± 1.0	0.53 ± 0.01
v06	188.3 ± 1.0	0.57 ± 0.01

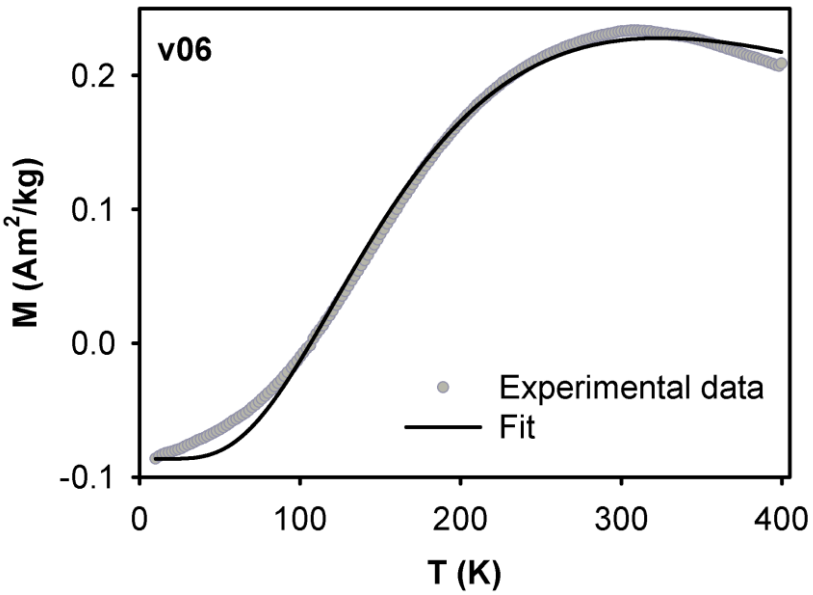

Figure S3: Example of the result of the ZFC curve refinement for the v06 nanocomposite sample.

Oxidation of butane to carbon dioxide

The catalytic activities of the nanocomposite samples were tested on butane gas oxidation to carbon dioxide in oxygen/argon atmosphere. A typical temperature profile of the reaction monitored by the MS is shown in Figure S4. The temperature dependence of the intensity of the CO_2-related peak in the MS experiment exhibit a maximum at around 250 ^{o}C for all investigated samples (summarized in Table S3) and it was assigned to the optimal temperature for the butane oxidation, T_c^{opt}. The working range of the catalyst is characterized by minimum, T_{min} and maximum, T_{max} temperature, corresponding to the onset and suppression of the oxidation, respectively. The values for all samples are summarized in Table S3.

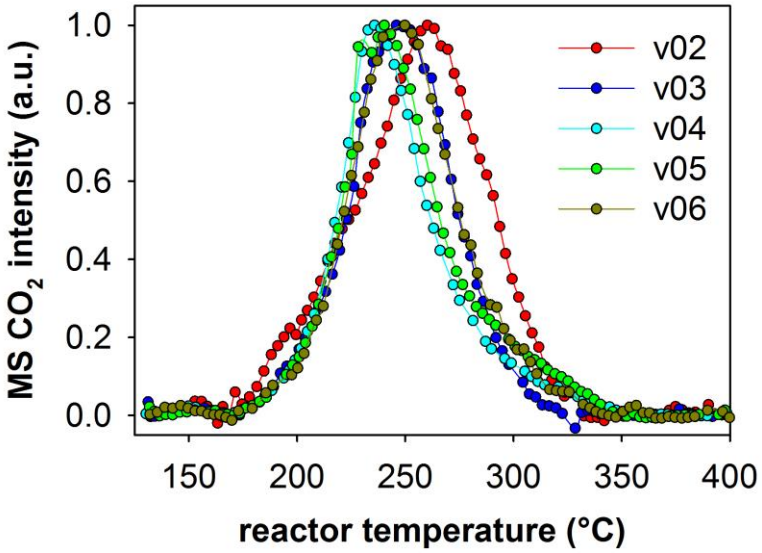

Figure S4: Temperature dependence of catalytic activity of samples prepared at various conditions.

For the samples prepared by slow adding of the NaOH, we observed that the optimal temperature, T_c^{opt} for the butane oxidation follows the trend of S_{BET} and d_{XRD}. However, the trend of the T_c^{opt} is opposite for the samples prepared by fast addition of the NaOH; the T_c^{opt} is increased up to 247°C for the sample v06 with the largest S_{BET} and lowest d_{XRD}.

The suppression of the catalytic activity is usually expected when the morphology of the catalyst is changed by the increased temperature. Consequently, the particle size increases or

additional process influencing the sample morphology (sintering, aggregation) or phase composition (inter-diffusion of ions, formation of high-temperature phases) takes place. Alternatively, the reaction mechanism may change. In order to clarify the observed character of the catalytic response, we performed analysis of the reaction products by the GC-MS. At temperatures above the T_c^{opt}, a mixture of organic compounds was detected with prevailing amount of acetone. Our observations are in good agreement with previously reported results [4]. Considering the results of the high-temperature PXRD experiment, the change of the reaction mechanism is the dominant factor responsible for suppression of the catalytic activity in butane oxidation as the particle size increased only moderately.

Table S3: Optimal temperature range for butane oxidation on the $CoFe_2O_4/CeO_2$_nanocomposite catalyst. The temperature corresponding to the maximum concentration of the CO_2, T_c^{opt} and the work range of the catalyst (T_c^{min} and T_c^{max}) is shown (range of error ~ 3°C).

Sample	T_c^{opt} **(°C)**	T_c^{min}**(°C)**	T_c^{max} **(°C)**
v02	259	162	338
v03	248	170	332
v04	239	171	345
v05	240	175	351
v06	247	171	340

Supplementary references

[1] M.F. Hansen and S. Morup, *J. Magn. Magn. Mater.*,199, **203**, 214-216.

[2] M. Knobel, W.C. Nunes, L.M. Socolovsky, E. De Biasi, J.M. Vargas and J.C. Denardin, *J. Nanosci. Nanotechnol.*, 2008, **8**, 2836-2857.

[3] M. El-Hilo, K. O'Grady and R.W. Chantrell, *J. Magn. Magn. Mater.*, 1992, **114**, 295-306.

[4] S. Scirè, S., Minicò, C. Crisafulli, C. Satriano, A. Pistone, *Appl. Catal. B: Enviromental* 2003, **40**, 43-49.